

Multifractal Spectrum of an Experimental (Video Feedback) Farey Tree

M. Piacquadio¹ and M. Rosen¹

Received May 31, 2004; accepted June 17, 2005

Published Online: March 7, 2007

A camera films a screen to which it is connected. It films its own image, feeding back the image to the screen. The camera can turn around an optical axis. A pattern of p light spots on the screen and q turns (feedback loops) of the camera appears, where p and q follow the hierarchy of a Farey tree. The Farey tree induces a measure distribution μ on the unit segment, different from the hyperbolic one μ^H induced by the Farey-Brocot interpolation. In this paper the multifractal spectrum of μ is studied and compared with that of μ^H ; the study of the latter spectrum is refined. The spectra are studied in this paper by means of different tools from Number Theory. The results of this study are interpreted in terms of p and q , empirically obtained in the video feedback experiment.

KEY WORDS: farey-tree, multifractality, Hausdorff measure, Number Theory

1. INTRODUCTION

A camera films a screen to which it is connected. It films its own image, feeding back the image to the screen. In the experiment, the camera can turn around an optical axis.⁽¹⁾ A pattern of p light spots on the screen and q turns (feedback loops) of the camera appears, where p and q follow the hierarchy of a Farey tree. A description of this experiment can be obtained from www.videofeedback.dk/world/ as well as the reference above. This is the first time a Farey tree has been observed as a sequence of spatial patterns, as previous observations of this hierarchy were made only in the temporal domain.

The nature of the findings is as follows: we obtain p light spots on the screen, after q feedback turns of the camera around its optical axis (this will be described in Sec. 17). Further, we obtain p' light spots, p' larger than p , after q' turns,

¹ Grupo de Medios Porosos, Departamento de Física, Facultad de Ingeniería, Universidad de Buenos Aires, Paseo Colón 850 (1063), Buenos Aires, Argentina; e-mail: gduitt@fibertel.com.ar.

$q' > q$. It is not possible to go, continuously, from situation p to situation p' . What happens between both situations is the appearance of $p + p'$ spots—for $q + q'$ turns, exactly. This is the nature of a Farey tree interpolation. Yet, it is not a Farey-Brocot (F-B) tree (as we will see below). Both trees induce measure distributions in the unit segment, as is possible to infer by looking at Fig. 2. The interpolation rules in that figure are the same: between rationals p/q and p'/q' , (p, q) and (p', q') relative prime, rational $(p + p')/(q + q')$ is strictly interpolated.

In this paper, we study both distributions, and we restrict ourselves to the unit interval. We decompose them by means of a multifractal spectral algorithm. The two spectra are complementary. A further objective of our paper is to interpret this complementarity in order to shed light on some aspects of the experimental results, as well as to connect them with key subjects in Number Theory.

The Farey-Brocot F-B and Farey-non-Brocot F-non-B (or simply F) trees appear time and again in a plurality of experiments in applied end empirical sciences. In this work we try to explore the mathematics underlying such universal problemata, by identifying and adapting some mathematical tools—which force us to somehow find a compromise between practicality and rigor. Our aim is to introduce mathematical notions of higher practicality than the known ones.

In the first part of this work, we will introduce some notation and elements of continued fractions (Sec. 2), Number Theory (Secs. 3–4), dimensionality and multifractality, which we will use throughout this paper. The observations in the optoelectronic experiment can be translated to key subjects in Number Theory language, via the multifractal decomposition formalism, and could be of help in order to (experimentally) explore the structure of the Lagrange spectrum, of which little is known, being only a partially solved problem in Mathematics.

In Secs. 2–4 we introduce tools from continued fractions, F-B interpolations, and leading problems in Number Theory, such as approximation of irrational numbers by rational ones, Jarnik classes and rings.

Dodson⁽²⁾ comments on the fact that, when dealing with dimensional issues, the sets involved are characterized by “lim sups.” We have reached similar conclusions: in Sec. 5 we characterize the Jarnik rings by means of a “lim sup” instead of the usual definition. In Sec. 6 we characterize the classical Markov irrationality index as a lim sup.

In *L'ordre dans le chaos*⁽³⁾ we read “...ce qui est important (*physiquement*) c'est ce qui a de la (*mesure*)...” In this paper we deal with two measure distributions, μ and μ^H , different from the usual Euclidean one: in Sec. 7 we review the concept of the multifractal spectrum $(\alpha, f(\alpha))$ of a measure, characterizing the α -concentration index for the F-B induced measure as a lim sup in Sec. 8.

This consistent replacement of “lim” by “lim sup” is due when working in a multifractal or multidimensional context, for such spectrum is given by a Hausdorff dimension, given in turn by a discontinuity of the Hausdorff measure,

which is defined on the basis of *coverings* of the set being measured, . . . hence, acting as an *exterior* measure.

In Secs. 10–11 we calculate the value of the theoretical spectrum $f_H(\alpha)$ for the minimal value α_{\min} of the α -concentration index of the measure induced by the F-non-B tree in the optoelectronic experiment. We use some results from Euler and a classical theorem of Dirichlet. In Secs. 12–13 we repeat the process with α_{\max} , using Liouville’s construction of irrationals of ultra-rapid growth to prove the existence of transcendental numbers. In Sec. 14.2 we describe the computational multifractal spectrum of the Farey-non-Brocot tree. In Sec. 14.3 we establish the relationship between the general α -concentration of this measure and the Jarnik rings (as redefined above). We compare the theoretical and computational spectra f_H and f_C . In Sec. 15 we complete the study of the F-B spectrum, relating the multifractal concentration index to the Markov irrationality index (as redefined above). In Sec. 16 we compare and relate the F-B and the experimental F-non-B multifractal spectra, showing that they are complementary.

Finally, in Sec. 17, we complete the description of the optoelectronic experiment, where we apply the concepts above indicated in order to shed light on the nature of the results.

1.1. The Thermodynamical Formalism or Multifractal Spectrum $(\alpha, f(\alpha))$: An Overview

In order to fix ideas, we consider the fractal Ω to be $[0, 1] = I$. A process in k -stages or steps subdivides I in finer and finer partitions of segments $l_i = l_i^{(k)}$. To each such segment a measure $\mu_k(l_i^{(k)})$ is associated, $\sum l_i \mu_k(l_i^{(k)}) = 1$. Examples of partitions are the F-B k -stages or the subdivision of I given by the evolution of the orbit of a grid of points under the action of a dynamical system. An example of μ_k probability measure on segments $l_i^{(k)}$ is the equimeasurability (i.e. the same measure) of all segments in an F-B k -step. Another example is the so called “natural measure” of a segment, as frequency or average of visitations of the orbit in the segment, at the k -stage of iteration of the dynamical system. Here, it is assumed that this frequency converges as k grows. In an empirical (or physics) context, there is no way to know whether this limit exists or not.

We introduce the α -concentration: the study of the density of a measure in a fractal $\Omega \subset [0, 1]$ poses a problem: let us take the 2^k segments of length $\frac{1}{3^k}$ in the k -stage of the construction of the ternary of Cantor K . In each such segment $l_i = l_i^{(k)}$, the Hausdorff measure of $K \cap l_i$ is $\frac{1}{2^k}$. So, the density of each l_i , that is, measure per unit length, is $(\frac{3}{2})^k$, which tends to ∞ as k grows. The *concentration*, or α -index,⁽⁴⁾ defined as the log-log version of the *density* would give $\frac{\log 2}{\log 3}$ for every segment $l_i^{(k)}$. The concept of average density on a segment and point-wise density have their corresponding α -concentration versions: $\alpha^{(k)}(l_i^{(k)}) = \frac{\log \mu_k(l_i^{(k)})}{\log l_i^{(k)}}$, whereas

$\alpha(x)$, $x \in I$, is defined by the limit of the $\alpha^{(k)}(l_i^{(k)})$, $x \in l_i^{(k)}$, as k grows, if that limit exists. Even for the so-called self-similar measures—the simplest possible of all examples—such limit fails to exist for a non-numerable infinity of points which are dense in $[0, 1]$ or in the fractal supporting the measure, and we find these problems in the context of this paper. We use the symbol $l_i^{(k)}$ for both the segment and its length.

It is to tackle such situations that physicists have developed the thermodynamical computational formal algorithm—or multifractal spectral decomposition—to be able to make sense out of, and extract relevant information from, numerical sequences that might not converge, limits that might not exist, magnitudes that could oscillate. Working at a certain k -stage, with the numerical data *available*, i.e. with $l_i^{(k)}$, μ_k , $\alpha^{(k)}$. . . the computational algorithm extracts from them, information relevant to the phenomenon under study, and to the associated process of distribution of weight, i.e. the would-be measure μ , *par abus de langage*. In fact, these are the limitations of our results, the context of our work: we work in stage k of F-non-B, and tackle the problem of oscillating magnitudes and non existence of limits.

We introduce the spectrum $f(\alpha)$: the formalism is still a gray zone, as we have no less than three definitions of it, as we briefly describe next. The spectrum $f(\alpha) = f_H(\alpha)$ is, by definition, the Hausdorff dimension of Ω_α , the set of all elements in Ω sharing the same α -concentration. The function $f_H(\alpha)$ is the so-called theoretical spectrum, “H” stands for “Hausdorff.” But, as we remarked, the limits involved might not exist. We stand at k -stage, and we assume, for simplicity, that we have a uniform partition: lengths of $l_i^{(k)}$ are $l^{(k)}$. If $N_\alpha^{(k)}$ denotes the number the segments $l_i^{(k)}$ for which $\alpha^{(k)}(l_i^{(k)})$ is—roughly—equal to α , then $\frac{\log N_\alpha^{(k)}}{\log \frac{1}{l^{(k)}}}$ is, for k large, the spectrum $f_C(\alpha)$, and the “C” stands for “computational.” When it exists, it yields an apparently smooth curve, its maximum being the fractal dimension of the underlying fractal, $f''(\alpha) \leq 0$, and other properties.

The advantage of f_C : it can yield such a smooth curve, without any limit whatsoever been proved to exist, e.g. in a completely empirical context where we deal, perforce, with a finite number of measurements—rendering meaningless the expression “ $k \rightarrow \infty$.”

The hope: f_H and f_C should coincide, should be the spectral decomposition of a certain measure.

The problem: it is exceedingly difficult to show when $f_H = f_C$, for which tentative distributions of measure on which fractals. . . In the present article we deal with this equality for the F-non-B case.

The importance: there is yet another definition of the multifractal spectrum: $f_L(\alpha)$, here “L” stands for “Lagrangian.” The algorithm expresses α and $f_L(\alpha)$, in terms of a parameter $q = f'(\alpha)$ —when the parameter is the derivative the coordinates are called Lagrangian. Magnitudes $q = f_L(\alpha)$, α , and $f_L(\alpha)$ can be

interpreted as inverse temperature, internal energy, and entropy⁽⁵⁾—hence the “thermodynamical formalism” notation—in a quantum mechanical context. That f_C , f_L , and f_H coincide has been proved for very few measure distributions in the literature.^(6–9) In this paper we do not deal with f_L , only with f_H and f_C for the F-non-B tree. When two multifractal spectra coincide, it is thought that the corresponding processes share subtle entropic/energetic relationships—perhaps not at all apparent. In this sense, it is remarkable that the spectra of the F-B and F-non-B trees, shown in Fig. 3, have no feature at all in common, despite the fact that both fractals $\Omega = [0, 1]$ coincide, and both interpolation rules are the same, i.e. adding numerators and denominators in near-neighbor rationals. The explanation of this fact lies in the nature of the α ’s in both spectra, the study of which is one of the aims of this paper.

2. CONTINUED FRACTIONS

2.1. Notation and Generalities

We will work with key tools in Number Theory, for which it is indispensable to consider each irrational number as expressed in its continued fraction expansion.

Some notation we will use consistently throughout this paper:

- (a) Let A, B, C_1 and C_2 be positive magnitudes. $A \sim B$, will signify: \exists constants C_1 and C_2 such that $C_1 B \leq A \leq C_2 B$.
- (b) $I = [0, 1]$ will be the set of real numbers between 0 and 1. Throughout this paper, we will work in I . With the letter “ i ” we will denote an irrational number in I , unless otherwise specified.
- (c) With $a_n, n \in \mathbb{N}$, we will denote a natural number, and

$$i = \frac{1}{a_1 + \frac{1}{a_2 + \frac{1}{\dots}}} = [a_1 \dots a_n \dots]$$

will be the continued fraction expansion of i , infinite in length.

- (d) The n -rational approximant to i will be

$$[a_1, \dots, a_n] = \frac{1}{a_1 + \frac{1}{a_2 + \frac{1}{\dots \frac{1}{a_n}}}} = \frac{p_n}{q_n}$$

- (e) With $a_n \equiv 1 \forall n$ we obtain the smallest possible $q_n = F_n$, the n th Fibonacci number, $F_n \sim \Phi^n$ where $\Phi = \frac{1+\sqrt{5}}{2}$, the golden mean. As we know, $\Phi \in I = [0, 1]$, and we work in I in this paper. Hence, we consider a version of Φ that belongs to I . With $a_n \equiv 2 \forall n$ we obtain the so-called silver mean.

2.2. Some Properties of $\frac{p_n}{q_n}$

It is easy to verify, with a few known examples, the following facts:

(i) $q_{n+1} = a_{n+1}q_n + q_{n-1}$.⁽¹⁰⁾

The q_n grow with n , this property and (i) imply that an irrational i is much closer to approximant $\frac{p_{n+1}}{q_{n+1}}$ than to $\frac{p_n}{q_n}$.

If $a_n \equiv 1 \forall n$, we obtain $i = [1, \dots 1, \dots] = \frac{\sqrt{5}-1}{2}$, the well known golden mean in $[0, 1] = I$, and in consequence equation (i) becomes $F_{n+1} = F_n + F_{n-1}$, which is the relationship between consecutive Fibonacci numbers.

(ii) If $\frac{p_{n+1}}{q_{n+1}} > \frac{p_n}{q_n}$ then $\begin{vmatrix} p_{n+1} & p_n \\ q_{n+1} & q_n \end{vmatrix} = 1$;

if $\frac{p_{n+1}}{q_{n+1}} < \frac{p_n}{q_n}$ then $\begin{vmatrix} p_n & p_{n+1} \\ q_n & q_{n+1} \end{vmatrix} = 1$.

This is a simple consequence of (i) and can promptly be verified with, say, the Fibonacci numbers, the Lucca numbers, the silver mean $s = [2, 2, \dots]$ or any other number we would like to try. The Lucca sequence goes like the Fibonacci F_n one, but with initial numbers $F_0 = 1$ and $F_1 = 3$ instead of $F_0 = 1$ and $F_1 = 1$. The silver means has $a_n = 2 \forall n$. A relationship between different means and Hyperbolic Geometry obtains in Ref. 11.

Property (ii) readily implies $dist(\frac{p_n}{q_n}, \frac{p_{n+1}}{q_{n+1}}) = |\frac{p_n}{q_n} - \frac{p_{n+1}}{q_{n+1}}| = \frac{1}{q_n q_{n+1}}$. The situation of i , $\frac{p_n}{q_n}$, and $\frac{p_{n+1}}{q_{n+1}}$ is as in Fig. 1a where we have i in between two consecutive rational approximants, and $dist(i, \frac{p_n}{q_n})$ is substantially larger than $dist(i, \frac{p_{n+1}}{q_{n+1}})$, so, as $n \rightarrow \infty$ the rational approximants tend to i . Therefore,

(iii) $dist\left(i, \frac{p_n}{q_n}\right) \sim dist\left(\frac{p_n}{q_n}, \frac{p_{n+1}}{q_{n+1}}\right) = \frac{1}{q_n q_{n+1}}$

We will work, throughout this paper, with properties (i) and (iii) with occasional call to (ii) *in every proof*.

(iv) If $i = [a_1, \dots, a_n \dots]$, then the rational approximant $[a_1, \dots, a_n] = \frac{p_n}{q_n}$ is obtained in the k F-B step, with $k = \sum_{j=1}^n a_j$.

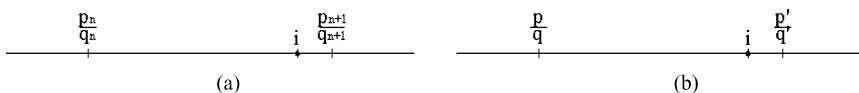


Fig. 1. The irrational number i between two nearby rationals.

3. THE FAREY-BROCOT (F-B) INTERPOLATION

The Farey tree interpolation—adding numerators and denominators—is ubiquitous in applied and empirical sciences, e.g. it appears in connection with resonance of systems where two frequencies compete.^(3,12) The optoelectronic experiment adds to the empirical context in which the tree appears. On the other hand, given an irrational number $i \in [0, 1]$, $i = [a_1, \dots, a_n, \dots]$, then $[a_1, \dots, a_n] = \frac{p_n}{q_n}$, $n \in \mathbb{N}$, are the rationals that best approximate i , and they are found, exactly in the k -level of F-B, with $k = \sum_{j=1}^n a_j$ ⁽¹³⁾. So, curiously, the Farey tree has to do both with the empirical sciences and with leading subjects in Number Theory, linking the latter to the former. This connection is explored in this paper with the aid of multifractal analysis.

Rational number $\frac{p+p'}{q+q'}$ is strictly interpolated between $\frac{p}{q}$ and $\frac{p'}{q'}$. Successive F-B interpolations in I are shown in Fig. 2a. There are 2^k segments in the k th partition. The F-non-B, or F interpolations are sketched in Fig. 2b. In Fig. 2a, for each k , a number is interpolated between two adjacent ones in step $k-1$. In Fig. 2b, the interpolation is made only if the denominator is no larger than the step.

Rationals $\frac{p}{q}$ and $\frac{p'}{q'}$, $\frac{p}{q} < \frac{p'}{q'}$, are adjacent in F-B for some F-B step or stage iff $|p'q - pq'| = 1$, in that case $dist(\frac{p}{q}, \frac{p'}{q'}) = \frac{1}{qq'}$. Notice that $\frac{p_n}{q_n}$ and $\frac{p_{n+1}}{q_{n+1}}$ from any $i = [a_1, a_2, \dots, a_n, \dots]$ do verify these properties akin to (ii) and (iii). Rational $\frac{p_n}{q_n}$ approximant to i is found in the F-B step $k = a_1 + a_2 + \dots + a_n$. Therefore, property (iii) can be seen as $dist(i, \frac{p_n}{q_n}) \sim \mu^L([\frac{p_n}{q_n}, \frac{p_{n+1}}{q_{n+1}}])$. Here μ^L is the usual Lebesgue measure.

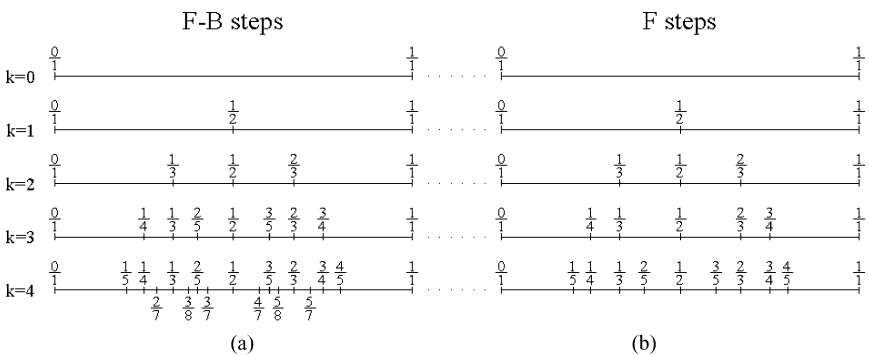


Fig. 2. Farey-Brocot and Farey-non-Brocot steps. We start this particular enumeration with $k = 0$, as we have zero interpolation in the initial step. We observe, in Fig. 2a, that a number is interpolated between two adjacent ones in the former step. Instead, from Fig. 2b, the interpolation follows the magnitude of the denominator.

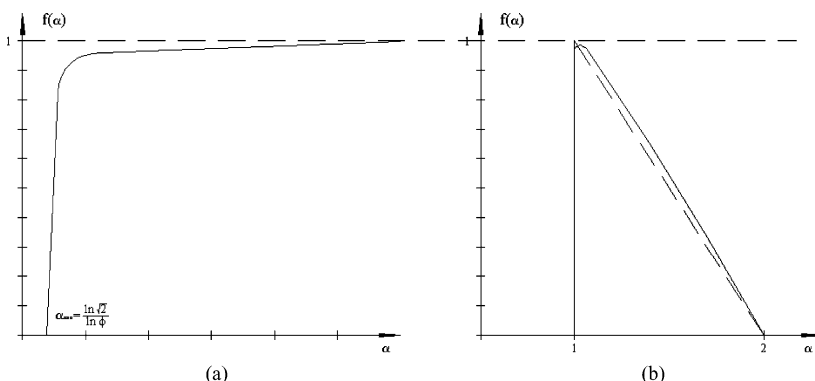


Fig. 3. In Fig. 3a, we have the strictly increasing F-B multifractal spectrum $f_H = f_C$. This type of spectrum has been termed “left-sided” by Mandelbrot. In Fig. 3b, the computational spectrum f_C for the experimental Farey tree, for a large value of the k -step.

4. RATIONAL APPROXIMATIONS TO IRRATIONAL NUMBERS

A leading subject in Number Theory is how near or far irrationals are from rational approximants. In order to tackle this subject, we will study the quantity $dist(i, \frac{p}{q})$, the distance between an irrational and rationals nearby. To that purpose we need to study the *Jarnik classes* which are, by definition:

$$J_{2+\sigma} = \left\{ i \text{ such that } dist\left(i, \frac{p}{q}\right) < \frac{1}{q^{2+\sigma}} \text{ for infinite values of } q \in \mathbb{N} \right\}.$$

Here σ is a non-negative number. For us, $\frac{p_n}{q_n}$ will be the rational $\frac{p_n}{q_n}$ from $[a_1 \dots a_n]$, where $i = [a_1 \dots a_n \dots]$. We recall $dist(i, \frac{p_n}{q_n}) \sim \frac{1}{q_n q_{n+1}}$. The $J_{2+\sigma}$ are ordered by inclusion, they are nested, as σ grows the $J_{2+\sigma}$ diminish. The largest class is J_2 , all I in it. Notice that, the larger σ is, the nearer i will be to its rational approximants. We want a disjoint version of the $J_{2+\sigma}$: we define the rings $G_{2+\sigma} = \cap_{\theta>0} J_{2+\sigma-\theta} - \cup_{\theta>0} J_{2+\sigma+\theta}$. Now, every i belongs to one and only one ring $G_{2+\sigma}$. In Refs. 14 and 15 we study the properties of $G_{2+\sigma}$. We give here a simplified idea of how an $i = [a_1 \dots a_n \dots] \in G_{2+\sigma}$ behaves: $G_{2+\sigma}$ is $J_{2+\sigma}$ worked upon, we take $J_{2+\sigma}$ and we weed out every i for which $dist(i, \frac{p_n}{q_n}) < \frac{1}{q_n^{2+\sigma+\theta}}$. We also pluck out every i for which such a distance is too often larger than $\frac{1}{q_n^{2+\sigma-\theta}}$. The result: such distance, for us $\frac{1}{q_n q_{n+1}}$, “behaves like” $\frac{1}{q_n^{2+\sigma}}$. The meaning of this “behaves like,” long and technical, is explained in Theorems 1 and 2 in Ref. 5, and we will pose $\frac{1}{q_n q_{n+1}} \sim \frac{1}{q_n^{2+\sigma}}$ or $q_{n+1} \sim q_n^{1+\sigma}$ for infinite values of n (a most simplified notion, but enough to give an idea of the evolution of the q'_n s).

Now $q_{n+1} \sim q_n^{1+\sigma}$ can be read $\frac{\ln q_{n+1}}{\ln q_n} \rightarrow 1 + \sigma$ for a certain subsequence $\{n_j\}$ of \mathbb{N} , that is $\frac{\ln q_{n_j+1}}{\ln q_{n_j}} \rightarrow 1 + \sigma$ when $j \rightarrow \infty$. But, if we took another sequence, still the logarithmic quotient cannot tend to a greater value $1 + \sigma + \theta$, for then we would have $i \in G_{2+\sigma+\theta}$.

We wonder if the sequence $\frac{\ln q_{n_j+1}}{\ln q_{n_j}}$ can oscillate. The answer is yes, in which case $\frac{\ln q_{n+1}}{\ln q_n}$ has no limit. We show next that, in this case, “lim” can be replaced by “lim sup.”

5. A DIFFERENT CHARACTERIZATION OF $G_{2+\sigma}$

5.1. Replacing “lim” by “lim sup”

We show first how $\frac{\ln q_{n+1}}{\ln q_n}$ can oscillate, then we analyze “lim sup” and “lim inf” of this oscillation. We conclude that “lim sup” is the relevant magnitude in order to characterize $G_{2+\sigma}$. Therefore, a simple way of characterizing $G_{2+\sigma}$ is: $i \in G_{2+\sigma}$ iff $\exists \{n_j\} \subset \mathbb{N}$ such that $\frac{\ln q_{n_j+1}}{\ln q_{n_j}} \rightarrow 1 + \sigma$ but, for any other subsequence, the limit cannot be larger than $1 + \sigma$. An even simpler way: $i \in G_{2+\sigma}$ iff $\limsup \frac{\ln q_{n+1}}{\ln q_n} = 1 + \sigma$.

An Oscillating Example

First we recall $q_{n+1} = a_{n+1}q_n + q_{n-1} = a_{n+1}q_n(1 + \frac{q_{n-1}}{q_n} \frac{1}{a_{n+1}}) = a_{n+1}q_n u$, u a close-to-unity magnitude.

Let us write $i = [a_1 \dots a_n \dots] = [1, 1, 1, a_{3 \times 1 + 1}, \dots, 1, 1, 1, a_{3j+j}, \dots]$ where $a_{3j+j} = q_{3j+j}^\sigma$. If we choose $n_j = 3j + j - 1$ we have $q_{n_j+1} = a_{3j+j}q_{n_j}u = q_{3j+j-1}^\sigma q_{n_j}u = q_{n_j}^{1+\sigma}u$. Then $\lim_{j \rightarrow \infty} \frac{\ln q_{n_j+1}}{\ln q_{n_j}} = 1 + \sigma$, the highest possible value of such limit, given therefore by $\limsup_n \frac{\ln q_{n+1}}{\ln q_n}$. This tells us that $i \in G_{2+\sigma}$. If we choose, on the other hand, $n_j = 3j + j - 2$, we have $a_{n_j+1} = 1$, from which we can deduce $\lim_{j \rightarrow \infty} \frac{\ln q_{n_j+1}}{\ln q_{n_j}} = 1 + 0$, the lowest possible value of such limit, hence $\liminf_n \frac{\ln q_{n+1}}{\ln q_n}$, which tells us $i \in J_{2+0}$, a trivial information. Therefore, “lim sup” is the relevant operation.

5.2. Dimensional Theorems

We saw that, if $\theta > 0$, σ as before, we have $J_{2+\sigma} \supset J_{2+\sigma+\theta}$, for $dist(i, \frac{p}{q}) < \frac{1}{q^{2+\sigma+\theta}} < \frac{1}{q^{2+\sigma}}$. Then we must have $\dim_H J_2 \geq \dim_H J_{2+\sigma} \geq \dim_H J_{2+\sigma+\theta}$. Here \dim_H stands for Hausdorff dimension. Hence, $\dim_H J_{2+\sigma}$ has to be a non-increasing function. Indeed, Jarnik⁽¹⁶⁾ proved $\dim_H J_{2+\sigma} = \frac{2}{2+\sigma} \forall \sigma > 0$. We will see later that $G_{2+\sigma}$ is dimensionally responsible for $J_{2+\sigma}$.

6. MARKOV'S IRRATIONALITY INDEX

For elements in J_2 , Markov introduced another way of studying distances between irrationals and their rational approximants. If $i = [a_1, \dots, a_n, \dots]$ then $\nu(i)$ is the *infimum* of values c such that $\text{dist}(i, \frac{p}{q}) \leq \frac{c}{q^2}$ for infinite values of q . Some authors^(17–18) use the better known $\overline{\nu(i)} = \frac{1}{\nu(i)}$. The magnitude $\overline{\nu(i)}$ is about quotients $\frac{1/q^2}{\text{dist}(i, p/q)}$ being as large as possible with large values that will hold for an infinity of q 's. We are computing $\limsup \frac{1/q^2}{\text{dist}(i, \frac{p}{q})}$. In our terms—and remembering that the sign “ \sim ” allows for multiplicative factors—this is: $\limsup \frac{1/q_n^2}{\text{dist}(i, \frac{p_n}{q_n})} \sim \limsup \frac{1/q_n^2}{1/q_n q_{n+1}} = \limsup \frac{q_{n+1}}{q_n} = \limsup \frac{a_{n+1}q_n + q_{n-1}}{q_n} = \limsup(a_{n+1} + \frac{q_{n-1}}{q_n}) \sim \limsup a_{n+1} = \limsup a_n$. Again, “lim sup” should be in the definition of Markov's irrationality index. The larger value of the multiplicative factor linking $\limsup(a_{n+1} + \frac{q_{n-1}}{q_n})$ with $\limsup a_n$ corresponds to the golden mean, where $a_n \equiv 1 \forall n$.

7. MULTIFRACTAL SPECTRA

We will deal with measures μ , always on $I = [0, 1]$, built in k -stages or approximation steps. Let us suppose we have I divided, in a certain k stage, in small segments—e.g. the 2^k segments in the k th step of the F-B algorithm shown in Fig. 2a. As k grows, the segments (in which I is divided) get smaller and smaller, the number of segments in stage k increases with k . We know the approximant measure μ_k of each segment in stage k . In what follows we will deal with $\alpha^{(k)}(i)$, $i \in I$ an irrational number.

8. THE MULTIFRACTAL SPECTRUM OF FAREY BROCAT (F-B)

8.1. The Origin of the Hyperbolic Measure in the Unit Segment

The hyperbolic half plane $\mathbb{H} = \{z = x + iy/y > 0\}$, endowed with the classical measure of Poincaré, has a tiling associated and a fundamental tile, such that the tiling covers \mathbb{H} , and that each tile is the fundamental one transformed by only one element of the unimodular group of transformations $U = \{z \rightarrow (az + b)/(cz + d), \det \begin{pmatrix} a & b \\ c & d \end{pmatrix} = 1; a, b, c, d \text{ integers}\}$. U is the set of rigid movements in \mathbb{H} . The hyperbolic measure of each tile is exactly the same as that of the fundamental tile. Surgery has been performed on the fundamental tile in order to yield another tiling whose tiles have virtual vertices in the real line \mathbb{R} , describing the Farey tree, starting to connect Hyperbolic Geometry to the tree.⁽¹⁹⁾ Still, the new fundamental tile is invariant under the action of two rotations in $U \dots$ so the new tiling is not representative of the set of rigid movements U .

Successive refinements of this surgery^(11,20) have produced a tiling of \mathbb{H} —with a fundamental tile—which does correspond to U , i.e. there is a different tile for each transformation in U applied to the fundamental tile. This tiling has two generators, matrices $L = \begin{pmatrix} 1 & 0 \\ 1 & 1 \end{pmatrix}$ and $R = \begin{pmatrix} 1 & 1 \\ 0 & 1 \end{pmatrix}$, with unity at the left and the right, respectively, of the matrix's diagonal. Let A be the only tile (in this particular tiling) with virtual vertices in 0 and 1 in the real line, i.e. associated to segment $[0, 1]$ —and, for short, let A be the corresponding transformation in U . The fundamental tile is the only one with virtual vertices in zero and infinity. Then tiles ALL , ALR , ARL . . . will be associated with segments $[0, 1/3]$, $[1/3, 1/2]$, $[1/2, 2/3]$, . . . So, matrices L and R act indeed as “left” and “right” describing the F-B partition in the unit segment. Words in letters L and R (but starting with A) with the same length have the same probability and, by extension, we have termed this measure in $[0, 1]$ as “hyperbolic,” so far in the literature So all 2^k segments in the k step of F-B have the same probability measure $1/2^k$. The irrational $i = [\alpha_1, \dots, \alpha_v, \dots]$ is covered, in the F-B step $\sum_{i=1}^n a_i$, by the segment with endpoints $\frac{p_{n-1}}{q_{n-1}}$ and $\frac{p_n}{q_n}$, and length $\frac{1}{q_{n-1}q_n}$, where the q 's are a function of the a 's, as described in Sec. 2.2. So the average α of that segment is $\alpha = \frac{\log 2 \sum_{i=1}^n a_i}{\log \frac{1}{q_{n-1}q_n}} = \log 2 \frac{\sum_{i=1}^n a_i}{\log(q_{n-1}q_n)} = \log 2 \frac{\sum_{i=1}^n a_i}{\frac{1}{n} \log(q_{n-1}q_n)}$ which shows that α depends on the average $\frac{\sum_{i=1}^n a_i}{n}$. The nature of the dependence of $\frac{1}{n} \log(q_{n-1}q_n)$ on $\frac{\sum_{i=1}^n a_i}{n}$ implies^(9,21) that α grows proportionally to the average. The condition $\frac{\sum_{i=1}^n a_i}{n}$ smaller than a certain maximal average M , yields nested growing sets as M grows, $\limsup_n \sum_n \frac{a_i}{n} = M$ yielding their disjoint versions. By choosing long rows of very small a 's the average $\frac{(\sum_{i=1}^n a_i)}{n}$ falls as low as we want. By adding next a sufficiently large a , the average grows as much as we want. By iterating this procedure, we can construct irrationals with the average oscillating between arbitrary magnitudes. The corresponding α will oscillate as well. We recall that the $J_{2+\sigma}$ are nested, the $G_{2+\sigma}$ being their disjoint version via a limsup argument, and that both $J_{2+\sigma}$ and $G_{2+\sigma}$ share the same fractal dimension—are equidimensional. The same argument yields equidimensional the sets arising from condition $\frac{\sum_{i=1}^n a_{ji}}{n} \leq M$ and $\limsup_n \sum_n \frac{a_j}{n} = M$.

We extend to the definition of α the limsup concept: we replace “lim” by “limsup” in the definition of the α index. The Ω_α are now well defined, disjoint, cover all the α -spectrum, and are defined for every $i \in [1, 0]$. Their dimension, $f(\alpha)$, tends to unity as α (and the corresponding value of M) grows, very rapidly, the difference $1 - f(\alpha)$ decreasing exponentially.^(9,20) The idea to estimate such $f(\alpha)$ is as follows: for $i = [a_1 \dots a_n \dots]$, let λ_j be the frequency with which the a 's are equal to j , $j \in \mathbb{N}$. Then we study the dependence of such frequencies on the average $\frac{\sum_{i=1}^n a_i}{n}$, identifying the key values $\bar{\lambda}_j$, $j \in \mathbb{N}$, corresponding to the maximal average associated with a certain value of α , i.e. responsible for the dimension $f(\alpha)$ of Ω_α .

The idea of treating a dimensional problem as a probability one, by expressing the magnitudes under study in terms of key frequencies, or proportions, or averages, and then identifying their key values, responsible for the solution, goes back to Good and Besicovitch.⁽²²⁾

This $f(\alpha)$ is the f_H theoretical spectrum. We have $f_H = f_C = f_L$ for the so-called “hyperbolic measure” in $[0, 1]$.

9. THE VIDEO FEEDBACK OPTOELECTRONIC EXPERIMENT

We briefly describe the optoelectronic experiment.⁽¹⁾ A camera films what is shown on a screen. In the screen we observe what the camera is filming, for camera and screen are connected as shown in Ref. 1. The camera can turn around its optical axis. Let us focus on Fig. 4a. The camera sees first a luminous spot. Then, when the camera turns an angle $\gamma = 120^\circ$, the spot appears in its new place on the screen while the first spot starts to fade out. A new turn with the same value γ produces now a third spot. The first one almost faded. The second one, starting to fade. A number of turns, always with the same value γ , yields a certain k number of feedback loops that ensures the stability of brilliance of the 3 spots. If p bright spots are seen on the screen, and q is the minimal number of feedback loops necessary to stabilize them, the corresponding angle γ involved is related to p and q by the equality $\gamma = \frac{2\pi}{p/q}$. So, p and q act as rational numbers.

Between spot-loop situations p/q and p'/q' , $p' > p$, $q' > q$, a $\frac{p+p'}{q+q'}$ one is observed, according to the hierarchy of the Farey-non-Brocot tree interpolation shown in the diagram of Fig. 4b. In that figure, the different levels of values of q denominators are separated, for when exploring e.g. a situation between $\frac{p}{q} = \frac{7}{2}$ and $\frac{p}{q} = \frac{11}{3}$, before performing $q = 9$ or 8 feedback loops (in order to see 32 or 29 spots) we must have done 5 loops (and have seen 18 spots). Further, we observe the distance between $\frac{7}{2}$ and $\frac{32}{9}$ adjacent in this tree (for they are adjacent in the F-B one): $dist(\frac{7}{2}, \frac{32}{9}) = \frac{1}{2 \cdot 9}$, whereas $dist(\frac{7}{2}, \frac{18}{5}) = \frac{1}{2 \cdot 5}$, so, larger denominators (of a higher level q) imply smaller incremental distances between the corresponding p/q rationals. And this means, in turn, smaller increments $\Delta\gamma$ between the corresponding angles $\gamma = \gamma(\frac{p}{q})$. But smaller increments $\Delta\gamma$ imply a greater level of precision when exploring the spot-loop situation.

10. THE MULTIFRACTAL SPECTRUM OF THE FAREY TREE

Let us recall that F_k is the k th level of interpolation in the experimental Farey tree. In Fig. 5 we see the $I^k(i)$ interval to which i belongs in the partition F_k , $k + 1 = q_n$. The length of $I^k(i)$ is $\frac{1}{q_n q_{n-1}}$. There are $\frac{3}{\pi^2} q_n^2 + O(q_n \log q_n)$ of such intervals covering I in F_k . This result, based on the Euler counting formula, is shown in Ref. 23.

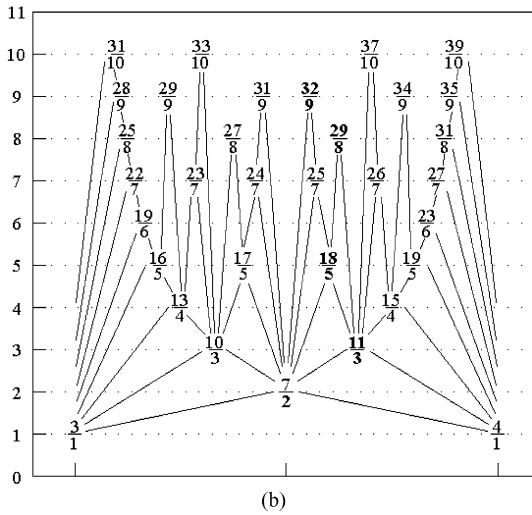
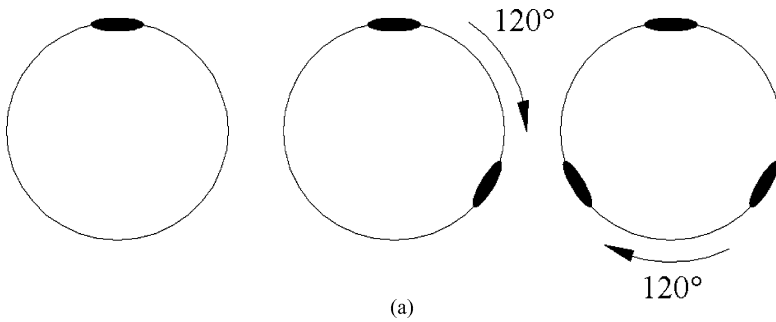


Fig. 4. Three bright spots on the screen, with an angle $\gamma = \pi/3$. The hierarchy of the Farey tree interpolation.

We will study the α -concentration (and the multifractal spectrum) of the measure distribution μ on I , induced by partitions F_k as $k \rightarrow \infty$. The approximation μ_k to μ will render as equimeasurable all segments of F_k . Let $i = [a_1 \dots a_n \dots]$ and choose $k + 1 = q_n$. The situation is as depicted in Fig. 5.



Fig. 5. The interval in the partition F_k to which the irrational i belongs.

We have $\alpha(i) = \lim_{k \rightarrow \infty} \alpha_k(i)$ where, by definition,

$$\begin{aligned} \alpha_k(i) &= \frac{\log \mu_k[I^k(i)]}{\log \mu^L[I^k(i)]} = \frac{\log\left(\frac{3}{\pi^2} q_n^2 + O(q_n \log q_n)\right)}{\log(q_n q_{n-1})} \\ &= \frac{2 \log q_n}{\log q_n + \log q_{n-1}} + \frac{\log\left(\frac{3}{\pi^2} + O(q_n \log q_n)/q_n^2\right)}{\log q_n + \log q_{n-1}} \end{aligned}$$

Now, as $k \rightarrow \infty$, the last numerator tends to $\log(3\pi^2)$, whereas both $\log q_n$ and $\log q_{n-1} \rightarrow \infty$, therefore we are left with

$$2 \frac{\log q_n}{\log q_n + \log q_{n-1}} = 2 \frac{1}{1 + \frac{1}{\frac{\log q_n}{\log q_{n-1}}}}$$

as a quantity relevant for $\alpha_k(i)$, $k + 1 = q_n$.

Now, $k \rightarrow \infty$ means $q_n \rightarrow \infty$ which only happens if $n \rightarrow \infty$. Therefore,

$$\alpha(i) = \lim_{n \rightarrow \infty} 2 \frac{1}{1 + \frac{1}{\frac{\log q_n}{\log q_{n-1}}}} = 2 \frac{1}{1 + \frac{1}{\lim_{n \rightarrow \infty} \frac{\log q_{n+1}}{\log q_n}}}$$

(if that limit exists).

Hence $\alpha(i)$ large (small) corresponds to i with $\frac{\log q_{n+1}}{\log q_n}$ large (small), where q_{n+1} is connected to q_n through the relation $q_{n+1} = a_{n+1} q_n + q_{n-1}$, as we recall.

11. THE THEORETICAL SPECTRAL VALUE $f(\alpha)$ FOR G_2

Let us consider the case $i \in G_2$. Now $G_2 = G_{2+\sigma}$ corresponds to $\sigma = 0$, and as we saw in Sec. 5.1, $\limsup_n \frac{\log q_{n+1}}{\log q_n} = 1 + \sigma = 1$. But, since $q_{n+1} > q_n$, we must have $\lim_{n \rightarrow \infty} \frac{\log q_{n+1}}{\log q_n} \geq 1$, the smallest possible value for such limit, which means that this limit exists without the ‘‘sup’’ and is equal to 1. Therefore, for every $i \in G_2$, we have $\alpha(i) = 2 \frac{1}{1+1} = 1$, the smallest possible value of α .

We calculate now the theoretical value $f(\alpha)$ for G_2 . We need $f(1) = \dim_H(G_2)$, for G_2 is the set of elements i sharing the same minimal value of the α -concentration. We will use a classical result of Dirichlet that states: for every i in I the inequality $\text{dist}(i, p/q) < 1/q^2$ holds for infinitely many values of q . With only Eqs. (i), (ii), (iii), we can see how natural this result is, for

$$\begin{aligned} \text{dist}\left(i, \frac{p_n}{q_n}\right) &< \frac{1}{q_n q_{n+1}} = \frac{1}{q_n(a_{n+1} q_n + q_{n-1})} \\ &= \frac{1}{q_n^2 a_{n+1} + q_{n-1}/q_n} < \frac{1}{q_n^2 a_{n+1}} \leq \frac{1}{q_n^2}. \quad (1) \end{aligned}$$

The q_n 's are infinite in number. It means that all irrationals in I are in J_2 , hence $\mu^L(J_2) = 1$. Now we need to weed out J_2 in order to obtain G_2 and find its

Hausdorff dimension. From the general definition of $G_{2+\sigma}$, we see that the case $\sigma = 0$ is different from the others: there are no $J_{2+\sigma-\theta}$ where

$$2 + \sigma - \theta < 2 + \sigma, \text{ so } G_2 = J_2 - \cup_{\theta>0} J_{2+\sigma+\theta} = J_2 - \cup_{\theta>0} J_{2+\theta},$$

so we can write

$$\begin{aligned} \mu^L(G_2) &= \mu^L(J_2) - \mu^L(\cup_{\theta>0} J_{2+\theta}) \\ &= \mu^L(J_2) - \mu^L(\cup_{n \in \mathbb{N}} J_{2+1/n}) \geq 1 - \sum_{n=1}^{\infty} \mu^L(J_{2+1/n}) = 1, \end{aligned}$$

we used the result by Jarnik:⁽¹⁶⁾ $\dim_H(J_{2+\theta}) = \frac{2}{2+\theta}$, $\theta > 0$. This result implies $\dim_H(J_{2+\theta}) < 1$ from which $\mu^L(J_{2+1/n}) = 0$. We are left with $\mu^L(G_2) = 1$, which certainly implies $\dim_H(G_2) = 1$, or $f(1) = 1$ for our spectral value. Notice that “1” is the maximal value that the multifractal spectrum $f(\alpha)$ may have since our irrationals are in \mathbb{R} , whose dimension is unity. So, our function $f(\alpha)$, with $\alpha \geq 1$, starts in $\alpha = 1$ with its own maximal value, hence it has to be decreasing.

12. THE MAXIMAL VALUE OF $\alpha(i)$

We had $\alpha(i) = 2 \frac{1}{1 + \frac{1}{\lim_{n \rightarrow \infty} \frac{\log q_{n+1}}{\log q_n}}}$, so, α is large iff the indicated limit is large.

Now, the obvious maximal value of such limit may be infinity: $i = [a_1, \dots, a_n \dots]$ has to have a growth so large as to ensure that $(\log q_{n+1})/(\log q_n)$ tends to infinity if n grows. In that case $\alpha(i) = 2$, the maximal possible value of α .

12.1. The Liouville Numbers

We now introduce a category of numbers: Liouville’s ultra-rapid growth numbers. An algebraic equation of n th degree is a polynomial of degree $n \in \mathbb{N}$ with integral coefficients, equated to zero. And an algebraic number of degree n is a real solution of an irreducible equation of the same degree. A classical result in Number Theory states that an algebraic number of degree $n \in \mathbb{N}$, $n \geq 2$, is in J_n , more specifically, in G_n . Liouville’s building of a transcendental (i.e. not algebraic) irrational $i = [a_1, \dots, a_n, \dots]$ is as follows: let $a_1 > 1$ be a natural number, $\frac{1}{a_1} = \frac{p_1}{q_1}$ the first approximant $[a_1]$ to an irrational number $i = [a_1 \dots a_n \dots]$ that we will build. Therefore $q_1 = a_1$, we pose $q_0 = 0$ and we define $a_2 = q_1^{(1)}$. Our second approximant to i is now

$$[a_1, a_2] = \frac{p_2}{q_2}, \quad \text{and } \text{dist} \left(i, \frac{p_2}{q_2} \right) \sim \frac{1}{q_2 q_1} = \frac{1}{q_1(a_2 q_1 + q_0)} = \frac{1}{q_1^3}.$$

Now, we pose $a_3 = q_2^2$ and we obtain

$$\text{dist}\left(i, \frac{p_3}{q_3}\right) \sim \frac{1}{q_2 q_3} = \frac{1}{q_2^2 a_3} \frac{1}{1 + \frac{q_1}{q_2} \frac{1}{a_3}} \sim \frac{1}{q_2^2 a_3} = \frac{1}{q_2^4}.$$

And, given q_n , posing $a_{n+1} = q_n^n$ we obtain $\text{dist}(i, \frac{p_n}{q_n}) \sim \frac{1}{q_n^{2+n}}$, which implies $i \in J_{2+n} \forall n$, hence $i \in J_\infty = G_\infty$. Therefore, such i cannot be an algebraic number, but a transcendental one. Let L be the set of Liouville numbers. Any i in L fulfills $\frac{\log q_{n+1}}{\log q_n} \rightarrow \infty$, and therefore, $\alpha(i) = 2$, the maximum possible value of α .

13. THE THEORETICAL SPECTRAL VALUE $f(\alpha)$ FOR ELEMENTS IN L

Since $L \subset G_\infty$, we have $\dim_H(L) \leq \dim_H(G_\infty) = \frac{2}{2+\infty} = 0$, by the Jarnik theorem in Sec. 5.2. Therefore, for $\alpha = 2$ we have $f(\alpha) = \dim_H(L) = 0$, which means: the spectral function for the measure induced by the Farey (non-Brocot) tree decreases from 1 to 0 as α increases from $\alpha = 1$ to $\alpha = 2$.

14. THE THERMODYNAMICAL FORMALISM

The theoretical spectrum $f(\alpha) = f_H(\alpha) = \dim_H(\Omega_\alpha)$, where Ω_α is the set of all elements sharing the same α -concentration, as we know, is *not* proved to be equal to the f_L obtained from the thermodynamical formalism. This algorithm feeds the computer in order to obtain a curve given by a function $f(\alpha) = f_C(\alpha)$ that—we hope—equals the theoretical spectrum. The articles which prove that the theoretical f_H and the computational f_C spectra coincide for this or that measure in I are few and far between: Refs. 6, 7 and 8 proved the equality for the so-called “self-similar” measures, whereas the corresponding equality for the hyperbolic μ^H measure on I was shown in Ref. 9. Now, both spectra $f(\alpha)$ are defined as limits, the same as α . But, when dealing with a computational algorithm, and with a measure constructed in k -steps or stages, like μ^H or μ , the expression “limit when the length of intervals in the k -step tends to zero” means simply “ $k \rightarrow \infty$ ” which, in computer language, means “ k as large as your computer can handle.” We call $f_C^{(k)}(\alpha)$ this computational spectrum.

14.1. The Hyperbolic μ^H Measure

In Ref. 9 we showed that $\lim_{k \rightarrow \infty} f_C^{(k)}(\alpha) = f_H(\alpha)$ for the spectrum associated with μ^H on I . Each $f_C^{(k)}(\alpha)$, $\forall k$, is endowed with every *theoretical* property of a *computational* spectrum. So, we have $(f_C^{(k)})'(\alpha) \leq 0$, the spectrum has an increasing branch, a maximum, a decreasing branch ... but, as k grows, the

increasing branch does not change much, while the decreasing one does: it stretches and goes to zero slower and slower. So $\lim_{k \rightarrow \infty} f_C^{(k)}(\alpha)$ has only an increasing branch, and the maximum is reached at $\alpha = \infty$.

14.2. The Measure Distribution μ Associated with the Experimental Farey Tree

For this measure distribution μ , built in k -stages, the corresponding $f_C^{(k)}(\alpha)$ have a non-positive second derivative as well, $\alpha \in [1, 2]$. But $f_C^{(k)}(\alpha)$, shown in Fig. 3b, is not strictly decreasing (as the theoretical $f_H(\alpha)$ has to be, as we learned at the end of Sec. 11). Around $\alpha = 1$ the function has a tiny increasing branch—that gets smaller and smaller as k grows—followed by a large decreasing branch which gets flatter and flatter as k grows, as if $\lim_{k \rightarrow \infty} f_C^{(k)}(\alpha)$ were a segment joining the theoretical values ($\alpha = 1; f(\alpha) = \dim_H(G_2) = 1$) and ($\alpha = 2; f(\alpha) = \dim_H(L) = 0$). We will interpret (below) this result in a theoretical way.

14.3. The Irrationals in $G_{2+\sigma}$

In the first place (Secs. 11–13), we notice that Ω_α with $\alpha = 1 = \alpha_{\min}$, is $G_2 = G_{2+0}$ exactly, whereas with $\alpha = 2 = \alpha_{\max}$, the Ω_α is G_∞ , a version of the Liouville set L . Therefore, with $\sigma = 0$ we are in α_{\min} , whereas with $\sigma = \infty$ we are in α_{\max} , which seems to suggest that, for intermediate values of σ , $0 < \sigma < \infty$, we are in intermediate values of $\alpha = \alpha(\sigma)$, $1 < \alpha < 2$: we need to explore a bit further the nature of irrationals $i \in G_{2+\sigma}$ for a general value of σ . We saw (Sec. 5.1) that a proper criterion to identify to which $G_{2+\sigma}$ a certain i belongs, is to calculate $\limsup_n \frac{\log q_{n+1}}{\log q_n} = 1 + \sigma$. Now, let us remember our definition of $\alpha \in [1, 2]$:

$$\alpha(i) = \lim_{k \rightarrow \infty} \alpha_k(i) = 2 \frac{1}{1 + \frac{1}{\lim_{n \rightarrow \infty} \frac{\log q_{n+1}}{\log q_n}}}$$

(if that limits exists). But the commonest situation, as we saw in Sec. 8, is that $\alpha_k(i)$ oscillates. In our case $\alpha_k(i)$ has a limit iff $\frac{\log q_{n+1}}{\log q_n}$ has a limit. But again, we saw in Sec. 5.1 how easy it is for $\frac{\log q_{n+1}}{\log q_n}$ to oscillate. Moreover, we saw that the dimensional information on i , i.e. to which $J_{2+\sigma}$ i does or does not belong, was given, exactly, by \limsup of the logarithmic quotient. Every other limiting value ($1 + \sigma'$, $\sigma' < \sigma$) of such quotient reiterates information we already know: $i \in J_{2+\sigma'}$, $\sigma' < \sigma$, which is trivial. If the dimensional information on i is given by

lim sup of the log quotient, then we may define

$$\alpha(i) = 2 \frac{1}{1 + \frac{1}{\limsup_{n \rightarrow \infty} \frac{\log q_{n+1}}{\log q_n}}} = 2 \frac{1}{1 + \frac{1}{1+\sigma}}.$$

We recall that, by replacing *lim* by *lim sup* in the definition of α in Sec. 8 we obtained desired results. We write now

$$\alpha(i) = 2 \frac{1}{1 + \frac{1}{1+\sigma}},$$

where $G_{2+\sigma}$ is the only Jarnik ring to which i belongs,

$$G_{2+\sigma} = \cap_{\theta > 0} J_{2+\sigma-\theta} - \cup_{\theta > 0} J_{2+\sigma+\theta}.$$

We remember that $J_{2+\sigma-\theta}$ is larger than $J_{2+\sigma}$, and has a greater dimension. By intersecting those $J_{2+\sigma-\theta}$ we get rid of *all* dimensions larger than that of $J_{2+\sigma}$. We conjecture here that the J 's, so rich in structure, have positive Hausdorff measure in their Hausdorff dimension, just as J_2 does. Hence, by subtracting all $J_{2+\sigma+\theta}$ we eliminate sets of dimension smaller than that of $J_{2+\sigma}$, in such a way that $G_{2+\sigma}$ has a dimension *exactly* like that of $J_{2+\sigma}$, i.e. $\dim_H(G_{2+\sigma}) = \frac{2}{2+\sigma}$. This implies

$$2 + \sigma = \frac{2}{\dim_H(G_{2+\sigma})}, \quad \text{or} \quad 1 + \sigma = \frac{2}{\dim_H(G_{2+\sigma})} - 1.$$

Replacing the last expression of $(1 + \sigma)$ in the value of $\alpha(i)$ above, we obtain:

$$\alpha(i) = 2 - \dim_H(G_{2+\sigma}) \forall i \in G_{2+\sigma} = \Omega_{\alpha(\sigma)}$$

where

$$\begin{aligned} \alpha(\sigma) &= 2 \frac{1}{1 + \frac{1}{1+\sigma}}. \text{ Since } \dim_H(G_{2+\sigma}) = f(\alpha(\sigma)), \text{ we have } f(\alpha) \\ &= 2 - \alpha \text{ for } \alpha \in [1, 2], \end{aligned}$$

which is exactly the segment joining points $(\alpha = 1, f(\alpha) = 1)$ with $(\alpha = 2, f(\alpha) = 0)$ which is the computational result.

Therefore, for the μ measure on I , the theoretical Hausdorff multifractal spectrum and the computational thermodynamical formalism coincide.

15. COMPARING BOTH FAREY SPECTRA

Next, we want to explore the comparison of both μ^H and μ spectra on I . We look first at what $i \in G_{2+\sigma}$, $\sigma, 0$, means for the a_n (and not for the q_n only). Using Eqs. (i), (ii) and (iii) it can be shown that condition $\limsup_n \frac{\log q_{n+1}}{\log q_n} = \sigma + 1$ can be rewritten as $\limsup_n \frac{\log a_{n+1}}{\log q_n} = \sigma$. This condition, with $\sigma > 0$, is incompatible (see

the Appendix) with bounded averages $A(n) = \frac{\sum_{i=1}^n a_i}{n} \leq const. \forall n$, which characterizes irrationals in Ω_α for the hyperbolic spectrum shown in Fig. 3a. Therefore, all elements in each such Ω_α are in $G_{2+\sigma}$ with $\sigma = 0$. Let $i = [a_1, \dots, a_n \dots] \in \Omega_\alpha = \Omega_{CM}$, C the constant of proportionality referred to in Sec. 8, that is $\limsup \frac{\sum_{j=1}^n a_j}{n} := \limsup A(n) = M$. In Sec. 6 we saw that $\bar{\nu}(i) \sim \limsup a_n$, let C^* be the corresponding proportionality constant. The condition “lim sup of the average equal M ” is readily seen as incompatible with $\limsup a_n < M$, hence $\bar{\nu}(i) \geq C^*M = C^*(\alpha/C)$, and $\liminf_{i \in \Omega_\alpha} \bar{\nu}(i) = \frac{C^*}{C}\alpha$ whence the Markov irrationality separates elements from different Ω_α .

16. JOINING THE μ^H AND μ SPECTRA

Now it makes sense to look at both spectra in Fig. 3. The μ^H one decomposes G_2 , which is the largest of all rings, i.e. the case $\sigma = 0$, whereas the μ one departs from G_2 with $\sigma = 0$ at the starting point, and then goes through every possible value of σ . The first spectrum increases, as we tend to encompass more and more elements in G_2 , the \dim_H tends to 1 (the corresponding \dim_H of G_2). The second spectrum is the complement of the first one: at the starting point $\alpha = 1, \sigma = 0$, we already arrived at the totality of G_2 with \dim_H already having reached unity. As σ grows the spectrum diminishes, for the $G_{2+\sigma}$ get smaller, encompassing fewer and fewer elements. In the first spectrum, α is given by extremal values of $\bar{\nu}$ ($\bar{\nu}$ is finite only in G_{2+0}). In the second one, we pass to other $G_{2+\sigma}$, and α is given by σ . Thus, both spectra are left-increasing and right-decreasing branches of a whole spectrum. Now, both $\bar{\nu}(i)$ and $\sigma(i)$ are a certain (extremal) relationship (a “lim sup”) between $dist(i, p/q)$ and $1/q$, which are two very small quantities when q is large. That is to say, both $\bar{\nu}$ and σ have to do with exploring how relatively small $dist(i, p/q)$ is. Or, how far or near an irrational i is from the rational p/q approximants to it. But this question is one of the leading subjects in Number Theory, and is encoded here, in our *whole* multifractal spectrum of the Farey algorithm.

17. CONNECTION WITH THE VIDEO FEEDBACK EXPERIMENT AND REALISTIC EXPERIMENTAL CONDITIONS

Now, we analyze the experiment considered:⁽¹⁾ the p and q (spots and feedback-loops respectively) when the camera turns around its optical axis an angle $\gamma = 2\pi/(p/q)$, in the neighborhood of a certain angle $\gamma = \gamma(i)$ associated with an irrational number i , which implies (p/q) near i . Further, we recall that, with a *small* increment $\Delta\gamma$, we obtain another p' and q' situation, with $p' > p, q' > q$, and $\gamma' = 2\pi/(p'/q')$ nearer $\gamma(i)$ than $\gamma = 2\pi/(p/q)$ is. Both (p/q) and (p'/q') are in the Farey tree shown in Fig. 2b at levels q and q' respectively, so that $|\frac{p'}{q'} - \frac{p}{q}| = 1$, and $dist(\frac{p}{q}, \frac{p'}{q'}) = \frac{1}{qq'}$. The situation is depicted in Fig. 1b.

So, we can express $i = [a_1, \dots, a_n, \dots], [a_1 \dots a_n] = \frac{p_n}{q_n}, n \in \mathbb{N}$, and consider $q_n = q, q_{n+1} = q' > q, p_n = p, p_{n+1} = p' > p$. Now, $\gamma = \frac{2\pi}{(p/q)}$ implies $\frac{p}{q} = \frac{2\pi}{\gamma}$, hence working in absolute values we have $\frac{2\pi}{\gamma^2} \Delta\gamma = \Delta(\frac{p}{q}) = |\frac{p'}{q'} - \frac{p}{q}| = \frac{1}{qq'} = \frac{1}{q_n q_{n+1}} \sim \text{dist}(i, \frac{p_n}{q_n})$. Since angles γ involved remain near $\gamma(i)$, the magnitude $\frac{2\pi}{\gamma^2}$ does not change. Hence, the smallness of increment $\Delta\gamma$ is given directly by $\text{dist}(i, p/q) = \text{dist}(i, p_n/q_n)$. But this distance, as we saw, is responsible for the $G_{2+\sigma}$ to which i belongs, hence, for the α -concentration $\alpha(i)$. To wit: let us consider irrationals corresponding to the decreasing spectrum $(\alpha, f(\alpha))$, i.e. $i \in G_{2+\sigma}, \sigma \geq 0, \alpha(i) = 2 \frac{1}{1+\sigma}$, and we fix a certain order of magnitude for the number q of loops. Then, the smaller $\alpha(i)$ is, the easier it is to find a good rational approximant to i with a not-so-fine increment $\Delta\gamma$ that corresponds to the real experimental conditions. Next, let $i \in G_2$, consider the increasing spectrum $(\alpha, f(\alpha))$, and fix a value of α in the domain of that spectrum. Again, we consider a certain fixed order of magnitude for q . Then, the higher Markov's $\nu(i)$ the easier it is to find a good rational approximant to i . "Easier" means, in this context, working with not-so-fine incremental values of $\Delta\gamma$, i.e. within the current experimental precision. Further, for this case $\sigma = 0$, this $\text{dist}(i, \frac{p_n}{q_n})$ given by $\Delta\gamma$ allows us to measure the Markov irrationality of i , so it is possible to estimate different elements of the Lagrange spectrum (the set of all Markov irrationalities) and the corresponding Hurwitz maximality (the supremum of the Lagrange spectrum).

18. CONCLUSION

The two spectra analyzed in this paper have a direct connection with the experimental results of the video feedback set-up, as shown in Sec. 17. Metrical properties of both multifractal spectra of the Farey tree (the increasing and the decreasing one) can be expressed in terms of angular increments $\Delta\gamma$ and spots and loops and vice versa. This experiment was the gateway in order to obtain the increasing-and-decreasing whole Farey multifractal spectrum. The α 's in both "halves" correspond to the well-known classifications—Dirichlet and Markov, Jarnik and Liouville—of Real Numbers in Mathematics. The observations in the optoelectronic experiment may be of help in order to (experimentally) explore the structure of the Lagrange spectrum, of which little is known, being only a partially solved problem in Mathematics.

APPENDIX: CHARACTERIZING IRRATIONALS IN THE HYPERBOLIC SPECTRUM

Condition $i \in \overline{A_m}$ means $\limsup \frac{\sum_{j=1}^n a_j}{n} = m$, which implies $\frac{\sum_{j=1}^n a_j}{n} \leq m + 1, \forall n$ large enough. Hence $\frac{a_{n+1}}{n+1} < \frac{\sum_{j=1}^{n+1} a_j}{n+1} \leq m + 1$ if n is large, or else

$a_{n+1} \leq (m+1)(n+1)$. Therefore

$$\begin{aligned} \frac{\log a_{n+1}}{\log q_n} &\leq \frac{\log(n+1)}{\log q_n} + \frac{\log(m+1)}{\log q_n} \\ &= \frac{\log(n+1)}{\log n} \frac{\log n}{\log q_n} + \epsilon(n), \epsilon(n) \rightarrow 0 \text{ if } n \rightarrow \infty. \end{aligned}$$

Since

$$q_n \geq F_n \cong \text{const } \phi^n, \text{ we have } \frac{\log n}{\log q_n} \rightarrow 0,$$

therefore

$$\frac{\log a_{n+1}}{\log q_n} \rightarrow 0 \text{ when } n \rightarrow \infty, \text{ hence } i \in G_{2+\sigma} \text{ with } \sigma = 0.$$

REFERENCES

1. B. Essevez Roulet, P. Petitjeans, J. E. Wesfreid and M. Rosen, Farey sequences of spatiotemporal patterns in video feedback. *Phys. Rev. E* **61**(4): 3743–49 (2000) (www.videofeedback.dk).
2. M. M. Dodson, Exceptional sets in dynamical systems and Diophantine approximation. arXiv:math:NT/0108210 V1, Los Alamos National Laboratory, xxx.lanl.gov (2001)
3. P. Berge, Y. Pomeau and C. Vidal, *L'ordre dans le chaos*. Collection Enseignements des Sciences, (Ed. Hermann, Paris, 1994).
4. T. C. Halsey, M. H. Jensen, L. P. Kadanoff, I. Procaccia and B. Schraiman, Fractal measures and their singularities: The characterization of strange sets. *Nucl. Phys. B (Proc. Suppl.)* **2**: 513–516 (1986).
5. M. Duong-Van, Phase transition of multifractals. *Nucl. Phys. B (Proc. Suppl.)* **2**: 521–526 (1987).
6. R. Cawley and R. D. Mauldin, Multifractal decompositions of Moran fractals. *Adv. Math.* **92**(2): 196–236 (1992).
7. R. Riedi and B. Mandelbrot, The inversion formula for continuous multifractals. *Adv. Appl. Math.* **19**: 332–354 (1997).
8. R. Riedi and B. Mandelbrot, Exception to the multifractal formalism for discontinuous measures. *Math. Proc. Camb. Phil. Soc.* **123**: 133–157 (1998).
9. M. Piacquadio and E. Cesaratto, Multifractal spectrum and thermodynamical formalism of the Farey tree. *Int. J. Bifurcation and Chaos* **11**(5): 1331–1358 (2001).
10. G. H. Hardy and E. M. Wright. *An Introduction to the Theory of Numbers*, Chap. I–IV (Clarendon Press, Oxford, 1938).
11. S. Grynberg and M. Piacquadio, Hyperbolic geometry and multifractal spectra. Part. II. *Trabajos de Matemáticas 252, Publicaciones Previas del Instituto Argentino de Matemáticas, I.A.M.-CONICET* (1995).
12. P. Cvitanovic, H. Jensen, L. P. Kadanoff and I. Procaccia, Renormalization, unstable manifolds, and the fractal structure of mode locking. *Phys. Rev. Lett.* **55**(4): 343–346 (1985).
13. C. Series, Non Euclidean geometry, continued fractions and ergodic theory. *Math. Intell.* **4**(1): 24–28 (1982).
14. M. Piacquadio Losada and S. Grynberg, Cantor staircases in physics and Diophantine approximation. *Int. J. Bifurcation and Chaos* **8**(6): 1095–1106 (1998).

15. S. Grynberg and M. Piacquadio, Self-similarity of Farey staircases. arXiv:math-ph/0306024 V1, Los Alamos National Laboratory, xxx.lanl.gov. (2003).
16. V. Jarník, Zur metrischen Theorie der Diophantischen Approximationen. *Prace Mat-Fiz* 91–106 (1928–29).
17. C. Series, The Markov spectrum in the Hecke group G_5 . *Proc. London Math. Soc.* **57**: 151–180 (1988).
18. A. Haas and C. Series, The Hurwitz constant and Diophantine approximation on Hecke groups. *J. London Math. Soc.* **34**: 219–234 (1986).
19. C. Series, The modular surface and continued fractions. *J. London Math. Soc.* (2) **31**(1): 69–80 (1985).
20. M. Piacquadio, The geometry of Farey staircases. *Int. J. Bifurcation and Chaos* **14**(12): 4075–4096 (2004).
21. E. Cesaratto and M. Piacquadio, Multifractal formalism of the Farey partition. *Revista de la Unión Matemática Argentina* **41**(2): 51–66 (1998).
22. L. J. Good, The fractional dimensional theory of continued fractions. *Proc. Cam. Phil. Soc.* **37**: 199–228 (1941).
23. G. H. Hardy and E. M. Wright. *An Introduction to the Theory of Numbers*, Chap. XVIII. (Clarendon Press, Oxford, 1938).